16

Small-Angle Neutron Scattering to Detect Rafts and Lipid Domains

Jeremy Pencer, Thalia T. Mills, Norbert Kucerka, Mu-Ping Nieh, and John Katsaras

Summary

The detection and characterization of lateral heterogeneities or domains in lipid mixtures has attracted considerable interest, because of the roles that such domains may play in biological function. Studies on both model and cell membranes demonstrate that domains can be formed over a wide range of length scales, as small as nanometers in diameter up to microns. However, although the size and shape of micron-sized domains are readily visualized in freely suspended vesicles, by techniques such as fluorescence microscopy, imaging of nanometer-sized domains has thus far been performed only on substrate-supported membranes (through, e.g., atomic force microscopy), whereas additional evidence for nanodomains has depended on indirect detection (through, e.g., nuclear magnetic resonance or fluorescence resonance energy transfer). Small-angle neutron scattering (SANS) is a technique able to characterize structural features on nanometer length scales and can be used to probe freely suspended membranes. As such, SANS shows promise to characterize nanometer-sized domains in model membranes. The authors have recently demonstrated the efficacy of SANS to detect and characterize nanodomains in freely suspended mixed lipid vesicles.

Key Words: Cholesterol; lipid membranes; membrane domains; rafts; small-angle scattering; unilamellar vesicles.

1. Introduction

The identification of putative functional domains or "rafts" in cell membranes has stimulated considerable study of the lateral organization of both cell and model membranes, in part because of the possible roles of these domains in biological processes such as immune response, synaptic transmission, and viral infection *(1)*. A variety of techniques have been used in order to characterize lateral heterogeneities in both model and cell membranes, including fluorescence

microscopy *(2)*, nuclear magnetic resonance *(2,3)*, electron paramagnetic resonance *(4)*, fluorescence correlation spectroscopy *(5)*, fluorescence resonance energy transfer *(6)*, single-molecule tracking *(7)*, atomic force microscopy *(8)*, near-field optical microscopy *(9)*, and small-angle neutron scattering (SANS) *(10)*. Of this variety of techniques, fluorescence microscopy appears to have gained the greatest popularity, whereas small-angle scattering has found the least use in characterizing membrane domains. The popularity of visually based techniques over scattering is likely a consequence of the relative complexity in the analysis and interpretation of scattering data. Nevertheless, despite these complexities, SANS has inherent advantage over visual techniques, in probing nanometer length scales, and yielding ensemble-averaged information. Additionally, SANS uses selective lipid deuteration as a method of contrast enhancement rather than the addition or inclusion of bulky fluorescent dyes or labels, which can perturb or affect the phase behavior observed by techniques such as, for example, fluorescence microscopy *(11)*.

The detection of domains using SANS depends on the use of contrast variation. First, contrast between domains of different composition is enhanced by the selective deuteration of a lipid that is known (or suspected) to preferentially partition into one phase (or type of domain) over the other. Second, the contrast between the vesicle and medium is minimized, through the appropriate ratio of H_2O to D_2O in the buffer medium. This minimum contrast condition occurs when the scattering length density (SLD) of the medium is equal to the mean SLD of the vesicle. When lateral segregation occurs, the domains or heterogeneities in the vesicles will now have SLD that are unequal to the mean SLD, resulting in contrast between these domains and the medium. As will be shown, both the angle dependence of the SANS curve, and its integrated intensity will contain information related to the size and composition of domains present on the vesicle.

2. Materials

2.1. Buffer Media

1. 99% Purity D_2O (Cambridge Scientific, Andover, MA).
2. Ultrapure H_2O.
3. Buffer media as required, with either NaOH or HCl for pH titration, as required.

2.2. Lipid Mixtures

1. Reagent grade chloroform (Sigma-Aldrich, St. Louis, MO).
2. Rotary evaporator (e.g., Buchi, Sigma-Aldrich) or pressurized inert gas (e.g., N_2, He, and Ar).
3. Phospho and/or sphingolipids (Avanti Polar Lipids, Alabaster, AL).
4. Cholesterol or other sterols (Sigma-Aldrich).

2.3. Rapid Solvent Exchange

1. Chloroform (e.g., Sigma-Aldrich).
2. Buffer media (e.g., Hepes, Sigma-Aldrich).
3. Vortexer (e.g., Vortexer Shaker Miniroto 115V, Fisher Scientific, Ottawa, ON).
4. Vacuum pump (e.g., Integrated Speedvac System, Fisher Scientific).

2.4. Extrusion

1. Nuclepore polycarbonate track-etch membranes (pore diameters 200, 100, and 50 nm).
2. Either a hand-held mini-extruder (e.g., Avanti Polar Lipids) or high-pressure extruder (Northern Lipids Inc., Vancouver, BC).
3. Pressurized inert gas (e.g., N_2, He, and Ar).

2.5. Small-Angle Scattering

1. 1-mm Path length quartz cuvets (Hellma USA, Plainview, NY).
2. Circulating water bath temperature control.
3. Multiple-position sample changer.

3. Methods

As discussed, the detection of lateral segregation in model membranes by neutron scattering relies on the labeling, by selective deuteration, of at least one lipid species in the lipid mixture. As will be shown, without deuteration, most lipids and sterols have very similar SLD, making them difficult to distinguish by neutron scattering. Furthermore, the detection of lateral segregation is optimal under contrast matching conditions, i.e., when the SLD of the medium equals the mean SLD of the vesicles. In order to obtain reproducible results, it is essential that unilamellar vesicles (ULVs) be prepared under conditions wherein the lipid components are homogeneously mixed. Should extrusion be performed on laterally segregated mixtures, it is likely that individual vesicles produced will have different proportions of the various lipids present. Homogeneous mixing of the lipid components during extrusion can be achieved by maintaining the lipid film at a temperature above the miscibility transition, wherein miscibility transitions are either known from the literature *(2)* or can be estimated from miscibility transitions for similar mixtures. As a general rule, complete mixing can be achieved by maintaining the mixture at a temperature about 10°C above the gel–fluid transition of the lipid component with the highest melting point.

3.1. Estimation of Contrast Matching Conditions

1. As will be shown, it is advantageous to prepare extruded vesicles at conditions close to their contrast match point. Contrast match conditions correspond to a situation wherein the SLD of the buffer or medium is equal to the mean SLD of the ULV, and can be achieved by varying the D_2O content in a $D_2O{:}H_2O$ buffer.

Table 1
Neutron Coherent Scattering Lengths
for Atoms Commonly Found in Lipid
Molecules

Atom	Scattering length (fm)
C	6.6460
H	–3.7390
D	6.671
N	9.36
O	5.803
P	5.13

From **ref. *12***.

2. The SLD (ρ) of a molecule can be calculated by:

$$\rho = (1/V)\sum b_i$$

where b_i is the scattering length of the *i*-th atom in the molecule and *V* corresponds to the molecular volume. The scattering lengths of all atoms and their isotopes can be found in a number of sources *(12)*. **Table 1** summarizes atomic scattering lengths for atoms commonly found in lipid molecules.

3. The mean vesicle SLD can be calculated similarly, as the sum of the scattering lengths of all the components, divided by the total vesicle volume. The mean vesicle SLD can also be expressed in terms of the sum of the SLD of the various lipids in the vesicle.

$$\overline{\rho} = \frac{\sum_j n_j b_j}{\sum_i n_j V_j} = \frac{\sum_j n_j V_j \rho_j}{\sum_i n_j V_j}$$

where n_j, b_j, V_j, and ρ_j are the molar fraction, scattering length, molecular volume, and SLD of lipids of type *j* making up the vesicle, whereas $\overline{\rho}$ is the mean vesicle SLD. **Table 2** lists neutron scattering lengths (*b*) molecular volumes (*V*) and SLD (ρ) of typical lipids.

3.2. Preparation of Lipid Mixtures by Rapid Solvent Exchange

1. A detailed discussion of the preparation of vesicles by rapid solvent exchange (RSE) can be found in **ref. *15***.
2. Dissolve the various lipids to desired concentrations (e.g., 10 mg/mL) in chloroform.
3. Mix the various lipid solutions in the desired proportions into a small vial.
4. Add the appropriate buffer or water solution to the lipid–chloroform solution.
5. Vortex the sample and pump under vacuum for approx 1 min.

Table 2
Neutron Scattering Lengths, Molecular Volumes, and Corresponding Scattering Length Densities of Common Lipids

Molecule	Chemical formula	b (fm)	V (Å^3)	SLD (fm/Å^3)
DPPC (20°C)	$C_{40}H_{80}NO_8P$	27.63	1144	0.024
DPPC (50°C)	$C_{40}H_{80}NO_8P$	27.63	1232	0.022
dDPPC (20°C)	$C_{40}H_{18}D_{62}NO_8P$	672.99	1144 (est.)	0.588
dDPPC (50°C)	$C_{40}H_{18}D_{62}NO_8P$	672.99	1232 (est.)	0.546
DOPC (30°C)	$C_{44}H_{84}NO_8P$	39.26	1303	0.030
Cholesterol	$C_{27}H_{46}O$	13.25	629	0.021
Water (25°C)	H_2O	−1.68	30	−0.056
Heavy water (25°C)	D_2O	19.15	29.9	0.64

Lipid and cholesterol volumes taken from **refs. 13** and **14**.

Data for H_2O and D_2O are also shown for comparison.

DPPC, 1,2-dipalmitoyl-sn-glycero-3-phosphocholine; dDPPC, 1,2-dipalmitoyl-d62-*sn*-glycero-3-phosphocholine.

For dDPPC, the molecular volumes given are estimated (est.) from corresponding values for DPPC.

3.3. Preparation of Lipid Mixtures by Film Deposition

1. Dissolve the various lipids to specific concentrations (e.g., 10 mg/mL) in chloroform.
2. Mix the various lipid solutions in the correct proportions either in a small vial, or if solvent is to be removed through rotary evaporation, in a round-bottom flask e.g. Sigma-Aldrich.
3. Remove solvent by evaporation, either by flowing a gentle stream of N_2 (or any other inert gas) over the lipid solution or by rotary evaporation.
4. Remove any remaining solvent by vacuum pumping for at least 2 h.
5. Heat lipid film to 60°C. Note that for lipids with melting transition temperatures higher than 50°C, higher temperatures may be required for complete mixing of lipid components.
6. Preheat buffer to 60°C.
7. Add buffer to lipid film and disperse by vortexing, making sure to maintain the lipid dispersion at approx 60°C.

3.4. Lipid Extrusion

1. Preheat extruder to 60°C.
2. Preheat two 250-μL Hamilton syringes (Hamilton Company, Reno, NV) to 60°C.
3. Assemble extruder with 200-nm pore diameter polycarbonate membranes.
4. Pass preheated buffer solution through extruder a minimum of three times.
5. Extrude lipid dispersion at least 11 times through a 200-nm pore diameter polycarbonate membrane. Note that extrusion through a hand-held extruder requires an odd number of passes through the extruder, to avoid cross-contamination with sample that has not been extruded.

6. Repeat **steps 2–4** using the extruded dispersion but now with a 100-nm pore diameter polycarbonate membrane, instead of the 200-nm pore diameter membrane.

7. Using the 100-nm pore diameter extruded dispersion, repeat **steps 2–4** using a 50-nm pore diameter polycarbonate membrane, extruding the dispersion at least 25 times.

8. It is important to make samples with a relatively high lipid:buffer ratio as neutron sources produce relatively weak beams for experiments, compared with X-ray sources. However, high lipid concentrations can make extrusion difficult resulting in higher loss of lipid on the polycarbonate membranes. Moreover, too concentrated a sample will also introduce added complications to the analysis of the SANS data, as the appropriate structure factor is needed to account for the inevitable intervesicle interactions. As a result, extruding lipid samples with concentrations more than 50 mg/mL is not recommended. After extrusion, samples should be diluted to yield final concentrations no higher than approx 20 mg/mL, in order to avoid intervesicle interactions.

3.5. Small-Angle Neutron Scattering

1. Inject the vesicle suspension into a quartz cuvet, or sample cell. Boron-free optical quartz cells are appropriate for this use, as boron is a neutron absorber. It is also very important to avoid introducing air bubbles into the sample, as air bubbles will also scatter neutrons, complicating data analysis.

2. For samples with less than about 80% D_2O content, a 1-mm path length cell is recommended to avoid multiple scattering from hydrogenated components.

3. The neutron wavelength (λ) and sample-to-detector distance used should be appropriately chosen such that the length scales probed span the ranges including the vesicle size and membrane thickness. For 30-nm radius vesicles, with a typical bilayer thickness (e.g., 4–5 nm), the optimum q ($4\pi \sin\theta/\lambda$, where θ is the scattering angle) range for SANS measurements is $0.003 < q < 0.3$ Å^{-1}. For example, the NG3 30-m SANS instrument at the National Institute of Standards and Technology Center for Neutron Research, this q range is achieved using a λ of 8 Å, and sample-to-detector distance of 13, 4, and 1.3 m **(16)**.

4. The sample holder and sample changer should be capable of being preheated or cooled, with the sample (or samples) in place to the desired temperature. Keep in mind that the equilibration of the sample may not occur at the same rate as temperature equilibration of the sample holder.

5. Typically, SANS measurements are performed using a two-dimensional detector utilizing commercial multiwire proportional counters (MWPC) (Model XYP 64 × 64−10, manufactured by (CERCA, Romans, France) of the type developed at the Institute Laue-Langevin (ILL). As vesicles in the scattering volume have no preferred orientation, the signal is radially averaged. Data are corrected for the detector response, empty cell scattering, and detector dark count. Then, the corrected data is put on the absolute scale using calibrated standards or based on the incident neutron flux, as described in **ref. 16**. Most neutron scattering facilities provide their own software that will automatically perform radial averaging and the various corrections to SANS data.

6. Hydrogen atoms have a large incoherent scattering cross-section. In practice, this means that any sample (including the buffer) that contains significant amounts of hydrogen will contribute to the incoherent background (i.e., an essentially flat, or q-independent baseline added to the signal of interest). As small-angle scattering curves typically decay very rapidly with increasing q, this flat background is most significant for data at large values of q. Thus, a good estimate for the incoherent background can be obtained from the value of the scattered intensity, measured at the highest q range of the experimentally obtained data. This value, corresponding to the incoherent background, is then subtracted from the experimental data.

3.6. Contrast Matching

1. The most reliable method for determining the contrast match point of vesicles is through contrast variation. Contrast variation relies on the use of a series of solvents having various proportions of H_2O and D_2O, and consequently, different SLDs.
2. First, prepare a stock ULV solution. The ULV should be made in a solution with an SLD close to or at the estimated contrast match point. This solution will then be used to prepare a series of ULV samples at different contrasts. Note that if the estimated contrast match point is within 20% of either 100% H_2O or D_2O, preparation of ULV in either pure H_2O or D_2O, respectively, is recommended, as, for example, a stock ULV solution in 90% D_2O could not be diluted to produce ULV in 100% D_2O.
3. Divide the ULV suspension into five equal volumes.
4. Prepare five stock solutions of different H_2O/D_2O ratios for dilution of ULV samples. Solutions should be prepared so that their dilution with the ULV samples yields five samples that are well spaced, with respect to their final D_2O (%) concentration. It is recommended that the H_2O/D_2O ratios of the stock solutions are determined such that dilution with the ULV suspensions yield final D_2O (%) concentration of $x \pm 20\%$ D_2O, $x \pm 10\%$ D_2O, and x, where x is the estimated contrast match point, in D_2O (%). If the estimated contrast match point is too close to either the 100% H_2O or D_2O conditions, then other contrasts (i.e., D_2O [%] solutions) may be used, as required.
5. Measure SANS curves for all five samples at 60°C. In order to properly evaluate the contrast match point, it is important that the SANS curves contain both a significant portion of the flat incoherent background (high q data) and low q, wherein the curve is insensitive to internal ULV structural variations. **Figure 1A** shows SANS curves taken for a single sample under various contrast conditions, before subtraction of the incoherent background.
6. Subtract the incoherent background from the SANS curves (as discussed earlier).
7. The zero-angle scattered intensity, $I(0)$, can be estimated from the intensity of the lowest value of q measured.
8. Plot $I(0)$ as a function of either the D_2O fraction or the SLD of the solution, ρ_s. $I(0)$, measured from a suspension of ULV is proportional to the square of the SLD contrast, $I(0) \sim (\bar{\rho} - \rho_s)^2$, where $\bar{\rho}$ is the mean vesicle SLD. Note that ρ_s is a linear function of D_2O (%). Thus, the minimum value of $I(0)$ yields the contrast
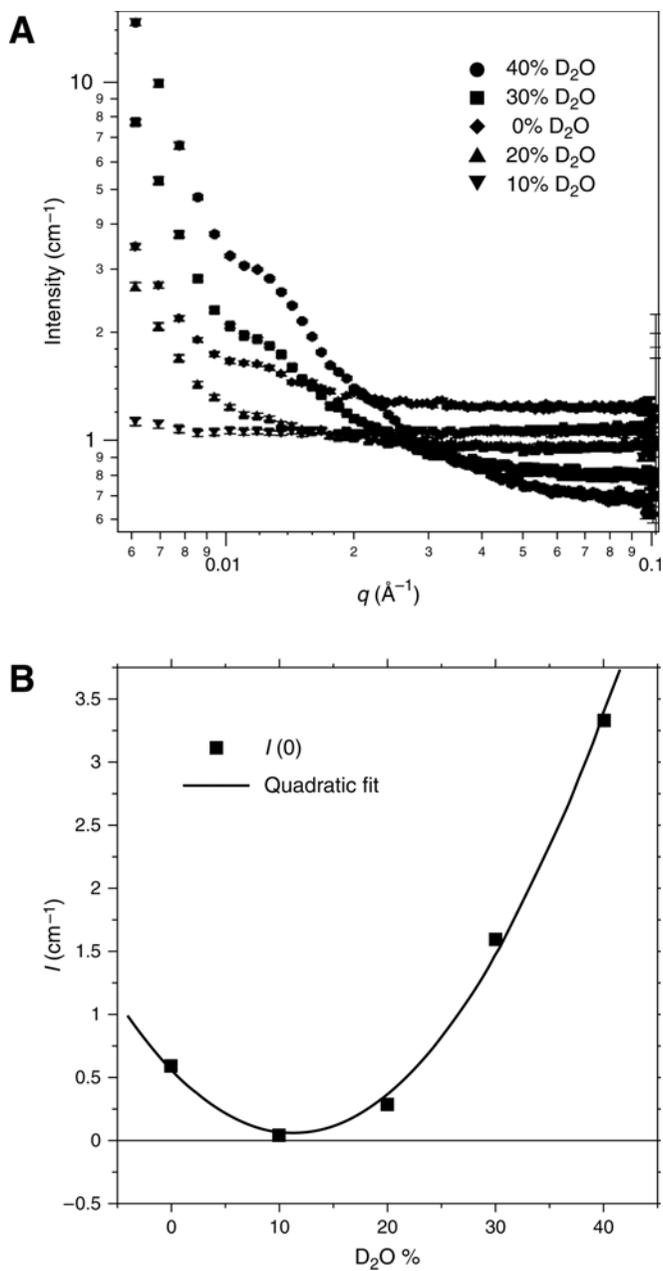
Fig. 1. **(A)** SANS curves plotted for 1:1:1 DOPC:DPPC:cholesterol ULV vs D_2O concentration in the buffer medium. **(B)** Zero-angle scattered intensity, $I(0)$, after subtraction of incoherent background, plotted as a function of D_2O fraction.

match point, or the vesicle's mean SLD, $\bar{\rho}$. A plot of $I(0)$ vs D_2O (%) is shown in **Fig. 1A**, along with a quadratic fit to the data.

3.7. Detection of Lateral Segregation

1. The scattering intensity from laterally heterogeneous vesicles can be expressed as a sum of three contributions:

$$I(q) = \left[F_{ave}(q) + F_{rad}(q) + F_{lat}(q) \right]^2$$

where $F_{ave}(q)$ is the scattering amplitude contribution from the mean vesicle SLD, $\bar{\rho}$, $F_{rad}(q)$ is the scattering amplitude contribution from radial fluctuations in the SLD (i.e., the difference between the acyl chain and headgroup SLD), and $F_{lat}(q)$ is the contribution to the scattered amplitude from lateral fluctuations in SLD (i.e., membrane domains). Typically, $F_{ave}(q)$ is the largest contribution to $I(q)$, except under contrast matching conditions, where $F_{ave}(q) = 0$. Thus, SANS measurements performed under contrast match conditions are optimal for measuring the contributions from $F_{rad}(q)$ and $F_{lat}(q)$.

2. Prepare a ULV sample at the experimentally determined contrast match point.

3. As there will be contributions to $I(q)$ from both F_{rad} and F_{lat}, it is recommended that at least one measurement be performed with ULV at high temperature, above the expected miscibility transition. This measurement will then show the contribution to $I(q)$ from $F_{rad}(q)$ alone, thus providing a baseline for possible temperature-dependent changes, owing to, for example, the onset of lateral segregation on cooling of the sample. **Figure 2B** shows $I(q)$ from laterally homogeneous vesicles at the contrast match point as a function of temperature. As can be observed from the figure, changes to $I(q)$, induced as a function of temperature, corresponding to changes in $F_{rad}(q)$, are small. Conversely, vesicles that become laterally heterogeneous on cooling show a dramatic change in $I(q)$ (shown in **Fig. 2A**), primarily because of the contribution from $F_{lat}(q)$.

4. Quantitative assessment of the degree of lateral segregation can be made by calculating the invariant, $Q = \int q^2 I(q) \mathrm{d}q$. As discussed in **ref. 17**, the invariant (Q) can be expressed (in analogy to $I[q]$), as a sum of three contributions:

$$Q = Q_0 + Q_{rad} + Q_{lat}$$

where Q_0 is the invariant contribution from $\bar{\rho}$, Q_{rad} is the contribution owing to the difference between the acyl chain and headgroup SLD, and Q_{lat} is the contribution from membrane domains. Q_0 and Q_{rad} can be measured experimentally or estimated with reasonable accuracy using known component scattering lengths and molecular volumes **(Table 2)** from the following relationships:

$$Q_0 = 2\pi^2 V \left(\bar{\rho} - \rho_s \right)^2 \quad \text{and} \quad Q_{rad} = 2\pi^2 \left[V_{ac} \left(\rho_{ac} - \bar{\rho} \right)^2 + V_h \left(\rho_h - \bar{\rho} \right)^2 \right]$$
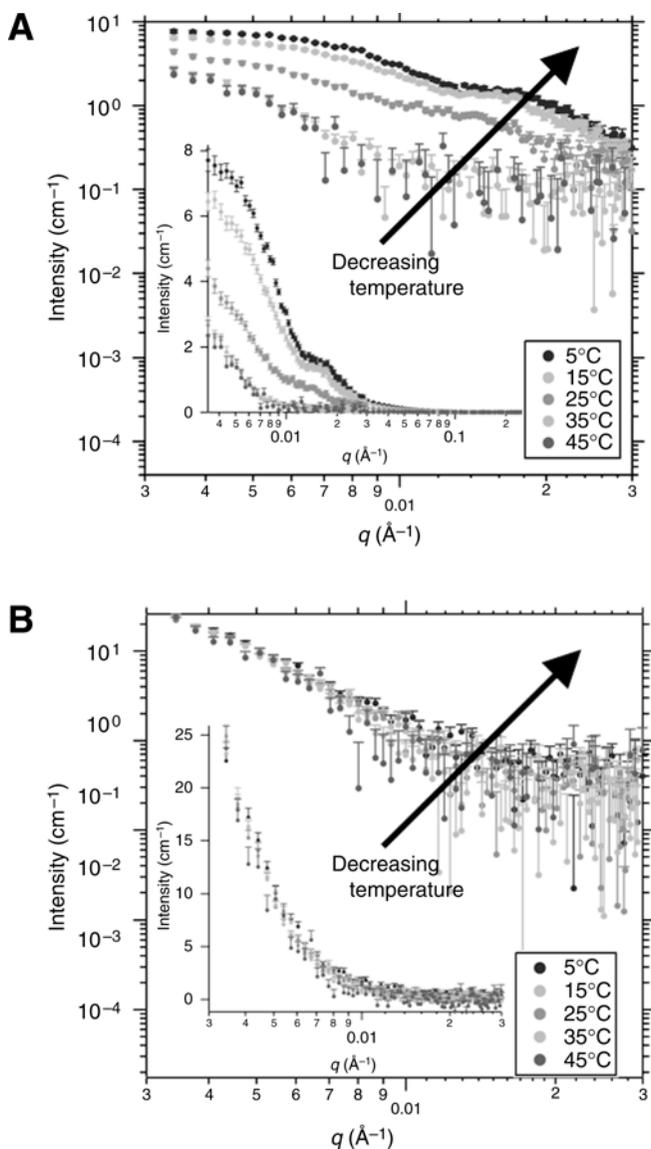
Fig. 2 **(A)** SANS curves plotted for 1:1:1 dDOPC:DPPC:cholesterol ULV vs temperature, under contrast matching conditions. **(B)** Similar curves plotted for 1:1:1 SOPC:dDPPC:cholesterol ULV vs temperature.

where Q_0 and Q_r are given with respect to a single vesicle, $V = V_{ac} + V_h$ is the total vesicle membrane volume, $\bar{\rho}$ is the vesicle mean SLD, ρ_s is the medium SLD, V_{ac} is the total membrane acyl chain region volume, ρ_{ac} is the mean acyl chain SLD, V_h is the total lipid headgroup region volume, and ρ_h is the mean headgroup SLD.
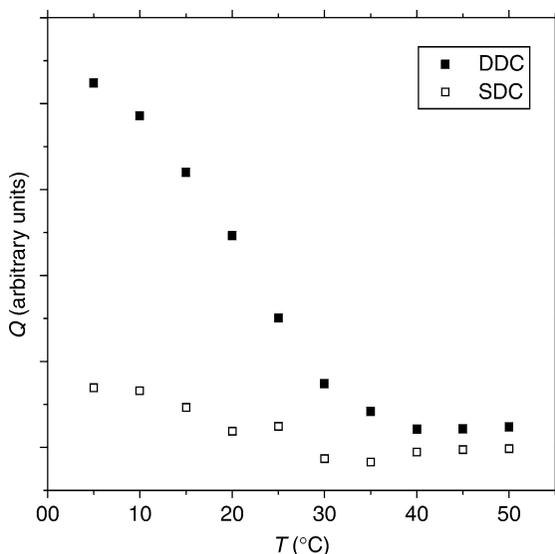
Fig. 3. The scattering invariant (Q) plotted vs temperature for 1:1:1 mixtures of DOPC:dDPPC:cholesterol (DDC) and SOPC:dDPPC:cholesterol (SDC). The data shown is normalized to lipid concentration.

5. Once Q has been calculated, $Q - Q_0 - Q_{rad}$ gives a quantitative indicator of the lateral segregation in the membrane. When the SLD of the lipid headgroups of the various components present in the membrane are the same then,

$$Q_f \sim a_1 \left(1 - a_1\right)\left(\rho_{1,ac} - \rho_{2,ac}\right)$$

where a_1 is the relative area fraction of regions 1 and $\rho_{1,ac}$ and $\rho_{2,ac}$ are the SLD of the acyl chain portions of regions 1 and 2. Q_f increases as the difference in SLD of the two regions increase and reaches a maximum value when either region 1 or 2 make half of the ULV surface.

6. **Figure 3** shows plots of Q vs temperature evaluated for the scattering curves shown in **Fig. 2A,B**.

3.8. Model-Dependent Analysis

1. If information is known either about the domain composition or relative area, it is possible to model the scattering by calculating the form factor of heterogeneous membranes. For example, in **ref. *10***, form factors for laterally homogeneous and heterogeneous vesicles are calculated by a Monte Carlo method, as described in detail in **refs. *18,19***.

2. In **Fig. 4** experimental data is shown, along with a coarse-grained model, constructed on the basis of known domain compositions and surface areas *(2)*. Using this coarse-grained model in combination with known compositions and area fractions, the authors were able to use SANS to assess the size and number of domains present in ULV.
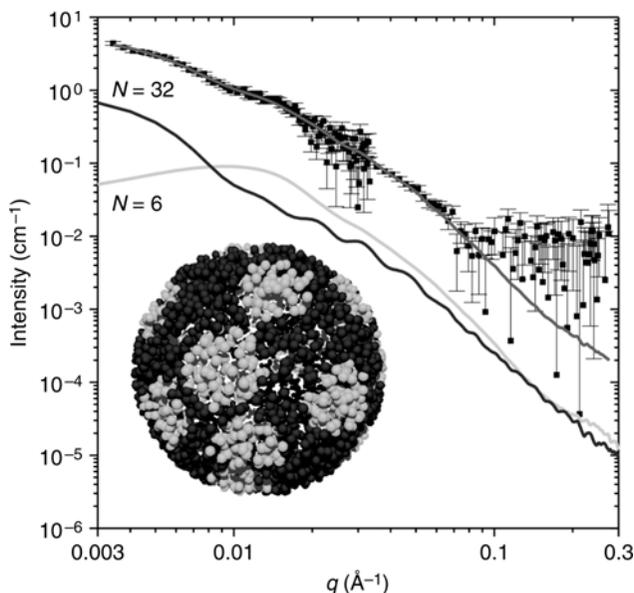
Fig. 4. SANS curve from DDC ULV at 25°C. The fit to the data, using coarse-grained modeling is shown (solid line) as well as curves calculated for ULV containing 6 or 32 domains. The inset shows a representative space-filling model of a vesicle with 32 domains.

4. Notes

1. There is some evidence in the literature that high membrane curvature may influence both the melting transition of single-component vesicles *(20)*, and the miscibility of lipids in multicomponent lipid mixtures *(21)*. Thus, the potential influence of membrane curvature should be considered when interpreting SANS data.

2. The RSE method produces MLV with low lamellarity (1–3 layers) compared with other methods, which produce MLV made up of hundreds of layers. Low lamellarity MLVs are easier to extrude through polycarbonate membrane pores, thus reducing the loss of lipid on the membrane. Thus, extrusion of vesicles prepared by the RSE method may increase yield and make the extrusion process easier, compared with extrusion of MLVs prepared by the hydration of lipid films.

3. The RSE method is also preferable to the film deposition method when using high sterol concentrations, because sterols such as cholesterol, might crystallize in dry lipid films above approx 45 mol% *(22)* or at much lower concentrations in the case of membranes containing polyunsaturated lipids *(23)*.

4. When lipid dispersions are extruded using a hand-held device, care should be taken to exert a slow and steady pressure on the syringe plungers during extrusion. If the lipid dispersion is pushed through the polycarbonate membrane of the extruder too quickly, there is a chance that the membrane will rupture, resulting in incomplete extrusion of the lipid dispersion.

5. For contrast matching, the zero-angle scattered intensity $I(0)$ can be estimated in several ways. As discussed, the intensity measured at the lowest scattering angle can be used to estimate $I(0)$. However, the scattering curves can be fit with the vesicle form factor and $I(0)$ can be determined as a fitting parameter, or the low-angle scattered intensity can be fit with a polynomial function and then extrapolated to obtain $I(0)$.

Acknowledgments

References

1. Edidin, M. (2003) The state of lipid rafts: from model membranes to cells. *Annu. Rev. Biophys. Biomol. Struct.* **32,** 257–283.
2. Veatch, S. L., Polozov, I. V., Gawrisch, K., and Keller, S. L. (2004) Liquid domains in vesicles investigated by NMR and fluorescence microscopy. *Biophys. J.* **86,** 2910–2922.
3. Polozov, I. V. and Gawrisch, K. (2004) Domains in Binary SOPC/POPE Lipid Mixtures Studied by Pulsed Field Gradient 1H MAS NMR. *Biophys. J.* **87,** 1741–1751.
4. Chiang, Y.-W., Shimoyama, Y., Feigenson, G. W., and Freed, J. H. (2004) Dynamic Molecular Structure of DPPC-DLPC-Cholesterol Ternary Lipid System by Spin-Label Electron Spin Resonance. *Biophys. J.* **87,** 2483–2496.
5. Kahya, N., Brown, D. A., and Schwille, P. (2005) Raft partitoning and dynamic behavior of human placental alkaline phosphatasein giant unilamellar vesicles. *Biochemistry* **44,** 7479–7489.
6. Silvius, J. R. (2003) Fluorescence energy transfer reveals microdomain formation at physiological temperatures in lipid mixtures modeling the outer leaflet of the plasma membrane. *Biophys. J.* **85,** 1034–1045.
7. Kusumi, A., Nakada, C., Ritchie, K., et al. (2005) Paradigm shift of the plasma membrane concept from the two-dimensional continuum fluid to the partitioned fluid: high-speed single-molecule tracking of membrane molecules. *Annu. Rev. Biophys. Biomol. Struct*. **34,** 351–378.
8. Yuan, C., Furlong, J., Burgos, P., and Johnston, L. J. (2002) The Size of Lipid Rafts: An Atomic Force Microscopy Study of Ganglioside GM1 Domains in Sphingomyelin/DOPC/Cholesterol Membranes. *Biophys. J.* **82,** 2526–2535.

9. Ianoul, A., Burgos, P., Lu, Z., Taylor, R. S., and Johnston, L. J. (2003) Phase Separation and Interleaflet Coupling in Supported Phospholipid Bilayers Visualized by Near-Field Scanning Optical Microscopy in Aqueous Solution. *Langmuir* **19,** 9246–9254.

10. Pencer, J., Mills, T., Anghel, V., Krueger, S., Epand, R. M., and Katsaras, J. (2005) Detection of submicron-sized raft-like domains in membranes by small-angle neutron scattering. *Eur. Phys. J. E* **18,** 447–458.

11. Veatch, S. L., Leung, S. S., Hancock, R. E., and Thewalt, J. L. (2007) Fluorescent probes alter miscibility phase boundaries in ternary vesicles. *J. Chem. Phys, B.* **111,** 502–504.

12. Sears, V. F. (1992) Neutron Scattering Lengths and Cross Sections. *Neutron News* **3,** 26–37.

13. Nagle, J. F. and Tristram-Nagle, S. (2000) Structure of Lipid Bilayers. *Biochim. Biophys. Acta* **1469,** 159–195.

14. Knoll, W., Schmidt, G., Ibel, K., and Sackmann, E. (1985) Small-Angle Neutron Scattering Study of Lateral Phase Separation in Dimyristoylphosphatidylcholine-Cholesterol Mixed Membranes. *Biochemistry* **24,** 5240–5246.

15. Buboltz, J. T. and Feigenson, G. W. (1999) A novel strategy for the preparation of liposomes: rapid solvent exchange. *Biochim. Biophys. Acta* **1417,** 232–245.

16. Glinka, C., Barker, J., Hammouda, B., Krueger, S., Moyer, J. J., and Orts, W. J. (1998) The 30 m Small-Angle Neutron Scattering Instruments at the National Institute of Standards and Technology. *J. Appl. Cryst*. **31,** 430–441.

17. Pencer, J., Anghel, V. N. P., Kučerka, N., and Katsaras, J. (2006) Scattering from Laterally Heterogeneous Vesicles I: Model Independent Analysis *J. Appl. Cryst*. **39**.

18. Henderson, S. J. (1996) Monte Carlo Modeling of Small-Angle Scattering Data from Non-Interacting Homogeneous and Heterogeneous Particles in Solution. *Biophys. J.* **70,** 1618–1627.

19. Zhou, J., Deyhima, A., Krueger, S., and Greguricka, S. K. (2005) LORES: Low resolution shape program for the calculation of small angle scattering profiles for biological macromolecules in solution. *Comp. Phys. Commun.* **170,** 186–204.

20. Gruenewald, B., Stankowski, S., and Blume A. (1979) Curvature influence on the cooperativity and the phase transition enthalpy of lecithin vesicles. *FEBS Lett.* **102,** 227–229.

21. Brumm, T., Jørgensen, K., Mouritsen, O. G., and Bayerl, T. M. (1996) The effect of increasing membrane curvature on the phase transition and mixing behavior of a dimyristoyl-sn-glycero-3-phosphatidylcholine/distearoyl-sn-glycero-3-phosphatidylcholine lipid mixture as studied by fourier transform infrared spectroscopy and differential scanning calorimetry. *Biophys. J.* **70,** 1373–1379.

22. Huang, J., Buboltz, J. T., and Feigenson, G. W. (1999) Maximum solubility of cholesterol in phosphatidylcholine and phosphatidylethanolamine bilayers. *Biochim. Biophys. Acta* **1417,** 89–100.

23. Shaikh, S. R., Cherezov, V., Caffrey, M., et al. (2006) *J. Am. Chem. Soc*. **128,** 5375–5383.